miR-500a-3p/CDK6 Axis Suppresses Aerobic Glycolysis in Colorectal Cancer

Yu Liu
Zhongshan Hospital Fudan University
wentao Tang
Zhongshan Hospital Fudan University
Li Ren
Zhongshan Hospital Fudan University
Tianyu Liu
Zhongshan Hospital Fudan University
Yang Meng
Tianjin Cancer Institute: Tianjin Tumor Hospital
Ye Wei
Zhongshan Hospital Fudan University
Yijiao Chen
Zhongshan Hospital Fudan University
Meiling Ji
Zhongshan Hospital Fudan University
Guosong Chen
State Key Laboratory of Molecular Engineering of Polymers
Wenju Chang
Zhongshan Hospital Fudan University
Jianmin Xu (xujmin@aliyun.com)
Zhongshan Hospital Fudan University https://orcid.org/0000-0001-5441-8240

Research Article

Keywords: Colorectal cancer, miR-500a-3p, CDK6, glycolysis

Posted Date: October 20th, 2021

DOI: https://doi.org/10.21203/rs.3.rs-991493/v1

Abstract

Backgrounds

Colorectal cancer (CRC) is one of the cancers with the highest mortality rate and understanding the mechanism behind its progression is the key to improve patients' prognosis. The role of miR-500a-3p has been demonstrated to be involved in the progression of several human cancers but its role in CRC is unclear. The aim of this study was to disclose the function of miR-500a-3p in CRC progression.

Methods

The expression of miR-500a-3p and Cyclin-dependent kinases 6 (CDK6) in 134 CRC tissues were tested respectively. The effects on cell proliferation by miR-500a-3p were explored in vitro and in vivo. The glycolysis of CRC cells was determined by Mass Spectrometry and Seahorse XF 96 Extracellular Flux Analyzer. Dual-luciferase reporter assay were performed to validate the relationship between miR-500a-3p and CDK6.

Results

miR-500a-3p was abnormally down-regulated in CRC tissues and cell lines and was negatively associated with malignancies and worse prognosis. miR-500a-3p mimics impeded CRC cells proliferation in vitro and in vivo. miR-500a-3p inhibited glucose consumption, lactate and ATP production, down-regulated the expression of hexokinase2 (HK2). Bioinformatics database prediction combined with western blot and luciferase assay confirmed that CDK6 is the direct target of miR-500a-3p. CDK6 overexpression was able to rescue the inhibitory function of miR-500a-3p on the proliferation and glycolysis in CRC cells.

Conclusions

The results of this study reveal a potential tumor suppressor role of miR-500a-3p by inhibiting proliferation and aerobic glycolysis through targeting CDK6 in CRC, which may provide new insights into novel prognostic biomarker and therapeutic targets for CRC.

Background

Colorectal cancer (CRC) is the third most commonly diagnosed cancer in the world with the second highest mortality rate[1]. The staging of tumor determines the prognosis of patients. 5-year survival ranges from greater than 90% in patients with stage I disease to slightly greater than 10% in patients with stage IV disease[2]. Therefore, understanding the mechanism behind the CRC progression is the key to improve patients' prognosis.

MicroRNAs (miRNAs) are a type of single-stranded non-coding RNA whose length are 21-25bp. miRNAs can regulate approximately 60% protein-coding genes[3]. Aerobic glycolysis, one of the central contributor to cancer progression[4], help cancer cell meet the energy demand, accumulate glycolytic intermediates for cancer biomass synthesis and create acidic microenvironment[5]. Existing studies have proved that microRNAs play an important role in the malignant progression of CRC by regulating key glycolytic genes directly or indirectly[6]. For example, miR-34a-5p inhibited CRC glycolysis via HK1 mediated glycolysis while miR-122-PKM2 axis attenuated glycolysis in CRC[7, 8]. miR-500a is located within the p11 locus on the X chromosome and plays various roles in tumors. It is upregulated in prostate cancer and promotes proliferation and invasion[9], and it promotes cell stemness via different pathways in gastric and liver cancer[10, 11]. But it suppresses cell proliferation, migration and invasion in non-small cell lung cancer[12]. According to the data of a 551 CRC patients' cohort from cBioportal database, miR-500a has the most significant correlation with prognosis (with the lowest *P* value). miR-500a has two arms. miR-500a-5p is down regulated and acts as a tumor suppresser in CRC. It could attenuate epithelial-mesenchymal transition through targeting the transforming growth factor-β signaling pathway[13] and suppress cell proliferation by targeting the p300/YY1/HDAC2 axis[14]. However, the role of miR-500a-3p has not been elucidated in CRC.

Cyclin-dependent kinases 6 (CDK6) is known as a classic cell cycle kinase that facilitates the progression of cells through the early G1 phase of the cell cycle. CDK6 can participate in the process of caner progression through its kinase-dependent or non-kinase-dependent function[15]. Recently, the role of CDK6 in metabolic regulation has been reported. Wang et al found that CDK6 could regulate the catalytic activity of two key enzymes in the glycolytic pathway, 6-phosphofructokinase and pyruvate kinase M2[16]. Nevertheless, the role of CDK6 in regulating CRC metabolism remains to be revealed.

In the current study, we studied the effects of miR-500a-3p on the proliferation and glycolysis of CRC in specimens and cell lines by targeting CDK6.

Results

miR-500a-3p is down regulated in tumor tissue and its low expression predicts poor prognosis

According to the data of a 551 patients' cohort from cBioportal database, we found that the expression of has-mir-500a was significantly associated with the prognosis of CRC patients (Supplementary Table 1) Patients who had low miR-500a expression had significantly poor overall survival (P=0.008, Supplementary Figure 1A) and progression-free survival (P<0.001, Supplementary Figure 1B). We firstly examined the miR-500a-3p expression in CRC cell lines, including HCT116, HT29, RKO, SW620, SW48 and SW480 and normal human colon epithelial cell line NCM460. miR-500a-3p was significantly down-regulated in CRC cells than that in NCM460 cells (Figure 1A). In addition, it was significantly down regulated in CRC tissues compared to nontumor tissues (Figure 1B). Next, we examined miR-500a-3p expression in a large CRC cohort and divided the patients into low-/high-expression groups by the cut-off of the median expression value. We found miR-500a-3p was negatively correlated with tumor size

(*P*=0.022) and differentiation (*P*=0.043) (Table 1). Survival analysis showed that low miR-500a-3p expression was significantly correlated with poor overall survival (*P*=0.0026, Figure 1C) and disease-free survival (*P*=0.0276, Figure 1D). To further evaluate the prognostic effect of miR-500a-3p, both univariate and multivariate analyses were performed. The results indicated that high miR-500a-3p expression is an independent protective factor for CRC [HR, 0.109; 95% confidence interval (CI), 0.014–0.875; *P*=0.037]. (Supplementary Table 2). We also analyzed the correlation of miR-500a-3p expression with cell proliferation protein (Ki-67) and glucose uptake marker (Standard Uptake Value, SUV) in CRC tissues. The expression of miR-500a-3p was significantly lower in the high ki67 group than that in the low ki67 group (Figure 1E). Besides, there was a negative correlation between the expression of miR-500a-3p and SUV with the *P* value of 0.038 and r value of -0.262 (Figure 1F). Altogether, miR-500a-3p low expression predicts poor prognosis in CRC patients and it may suppress CRC by regulating tumor proliferation and glucose metabolism.

miR-500a-3p suppress CRC growth in vitro and in vivo

HCT116/SW480 were transfected with miR-500a-3p mimics to investigate the function of miR-500a-3p. Transfection efficiencies were confirmed by qRT-PCR (Supplementary Figure 2A). CCK-8 and colony formation assays indicated that CRC cell proliferation and colony formation were significantly inhibited by miR-500a-3p (Figure 2A-D). Next, fluorescence-activated cell sorting (FACS) analysis revealed an increase in G1-phase cells and a concomitant decrease in S-phase cells by miR-500a-3p (Figure 2E, F). Then. we found that miR-500a-3p mimics did not promoted apoptosis significantly (Supplementary Figure 2B). Transwell assay showed that the miR-500a-3p mimics markedly inhibited CRC cell invasion (Supplementary Figure 2C). We established a xenograft tumor model with SW480 and HCT116 cells stably overexpressing miR-500a-3p (Supplementary Figure 2D-E). The mean volume and weight of tumors were lower in miR-500a-3p overexpression group than vector group (Figure 2G-I and Supplementary Figure 2F-H). The protein expression of cell proliferation (Ki-67) in the xenograft tumors was lower in miR-500a-3p overexpression group than vector group (Figure 2J). Altogether, these results indicated that miR-500a-3p suppress CRC cell proliferation in vitro and in vivo.

miR-500a-3p suppresses aerobic glycolysis in CRC

The expression of miR-500a-3p in CRC patients is negatively correlated with glucose uptake, indicating that miR-500a-3p may have an inhibitory effect on glycolysis. Cellular glycolytic activity was measured. As a result, miR-500a-3p significantly decreased glucose uptake (Figure 3A), lactate production (Figure 3B) and intracellular ATP levels (Figure 3C) in HCT116 and SW480 cells. The extracellular acidification rate (ECAR), measured by Seahorse analyzer, was downregulated by miR-500a-3p (Figure 3D). Furthermore, targeted metabolomics focused on the energy metabolism pathway were performed, and less level of glycolytic metabolites like glucose 6-phosphate, fructose 6-phosphate, fructose 1,6-bisphosphate, dihydroxyacetone phosphate and 3-phospho-glycerate caused by overexpression of miR-500a-3p was found. (Figure 3E and Supplementary Figure 3A-E). We then measured the expression of major genes involved in the glucose transport and glycolysis. miR-500a-3p mimics reduced the RNA level

of *HK2, PFKP, PGK1* and *LDHA* (Figure 3F) and the protein level of GLUT1, HK2 and PKM2 (Figure 3G). The protein expression of HK2 whose RNA and protein were both downregulated by miR-500a-3p was evaluated in the CRC cohort. It was negatively correlated with the miR-500a-3p levels (r=-0.418, *P*<0.0001, Figure 3H-I), confirming the negative regulation of HK2 by miR-500a-3p in CRC tissues. These data suggest that the overexpression of miR-500a-3p causes a decrease in glucose metabolism via altered regulation of multiple genes involved in glycolysis.

CDK6 is the direct target and down regulated by miR-500a-3p

To explain the mechanism of miR-500a-3p inhibiting the proliferation and glycolysis of CRC, we firstly used the publicly available algorithms TargetScan and miRDB to find the potential binding sites of glycolytic enzymes, like HK2, PFKP, PGK1 and LDHA, that down-regulated by miR-500a-3p. However, their 3'UTR did not have conserved binding site of miR-500a-3p, indicating it may regulate glycolysis indirectly (Supplementary Figure 4). CDK6, a novel glycolysis regulator[16], was predicted as a target of miR-500a-3p by TargetScan and miRDB database (Figure 4A). qPCR and Western blotting analysis showed that miR-500a-3p could reduce both the RNA and the protein level of CDK6, indicating that CDK6 may act as downstream targets of miR-500a-3p (Figure 4B-C). To further confirm this, we constructed two pair of luciferase reporter plasmid containing the predicted seed sequence of miR-500a-3p in the 3'-UTR of CDK6 mRNA and a control reporter containing the mutated sequence of the same fragment (Figure 4D). miR-500a-3p significantly inhibited the luciferase activity in cells containing the wild type CDK6 sequence, instead of the mutant sequence (Figure 4E-F). Finally, we evaluate CDK6 protein level in clinical CRC samples using IHC (Figure 4G), and a significant negative correlation was revealed between miR-500a-3p and CDK6 protein expression (r=0.0012, *P*=-0.285, Figure 4H). Collectively, these findings suggest that CDK6 is direct target of miR-500a-3p in CRC.

CDK6 is upregulated and promotes aerobic glycolysis in CRC

We firstly examined CDK6 protein level in 20 paired human CRC tumor and adjacent nontumor tissues using IHC (Figure 5A). The IHC staining results revealed that it was significantly up regulated in CRC tissues compared to nontumor tissues (Figure 5B). Survival analysis of the large CRC cohort showed that high CDK6 expression was significantly correlated with poor overall survival (*P*=0.0333, Supplementary Figure 5A) and disease-free survival (*P*=0.0559, Supplementary Figure 5B). CCK-8 and cell cycle assays indicated that CDK6 enhanced CRC cell proliferation (Supplementary Figure 5C and D). Then, we explored the influence of CDK6 on the aerobic glycolysis of CRC cells. As exhibited in Figure 5C-F, CDK6 promoted glucose uptake, the production of lactate and ATP and the ECAR in SW480 cells. The expression of major genes involved in the glucose transport and glycolysis were also measured. The RNA level of *GLUT1, LDHB, HK1* and *HK2* and the protein level of GLUT1, HK2 were elevated after CDK6 overexpressed (Figure 5G and H). In CRC tissues, the IHC score of HK2 was positively correlated with that of CDK6 (r=0.411, *P*<0.0001, Figure 5I). These findings indicated that CDK6 plays a role in promoting aerobic glycolysis in CRC.

miR-500a-3p mediates the inhibition in proliferation and aerobic glycolysis of CRC cells through targeting CDK6

To address whether miR-500a-3p exerted its role through targeting CDK6, we conducted rescue experiments. The CCK-8 and colony formation assays showed that CDK6 could promote CRC cell proliferation and colony formation and could eliminate the inhibition caused by miR-500a-3p (Figure 6A and B). As shown in Figure 6C, CDK6 overexpression counteracted the inhibitory effect of miR-500a-3p on the cycle of CRC cells. We explored the influence of miR-500a-3p/CDK6 axis on the aerobic glycolysis of CRC cells through measuring glucose uptake, lactate production, intracellular ATP level and ECAR. The inhibition of glycolysis caused by miR-500a-3p could be partly eliminate by CDK6 overexpression (Figure 6D-G). Together, these results indicated that miR-500a-3p suppressed CRC proliferation and aerobic glycolysis through down-regulating CDK6.

Materials And Methods

Patients

From January 2015 to March 2015, 134 continuous CRC specimens and 20 matching adjacent non-tumor specimens that obtained from CRC patients at the Zhongshan Hospital, Fudan University were collected. None of the patients received any preoperative chemotherapy or radiation. All tissue samples were pathologically diagnosed. The study was authorized by the Ethic Committee of the Zhongshan Hospital, Fudan University. Written informed consent was obtained from every patient.

Collection of TCGA public data and identification of significantly differential expression miRNA

We collected gene expression profiles of 551 COADREAD samples from TCGA cohort (http://gdac.broadinstitute.org/). Data including mRNA expression level and miRNA expression level. All the data have been standardized. For miRNAs differential analysis, we calculated the mean expression level of these miRNAs to divide them into high and low expression groups.

The R package DESeq2 (version 1.22.2) were used to calculate the differential expressed t statistics for microarray and RNA sequencing data. We used univariate Cox proportional hazards model to examine the associations between gene expression and overall survival. MiRNAs with P values less than 0.05 were considered to be statistically significant and included in consensus survival analysis.

Immunohistochemistry staining

Total 134 CRC specimens were stained with the CDK6 antibody (ab124821, Abcam) and HK2 antibody (2867T, Cell Signaling Technology). The 20 matched adjacent non-tumor specimens were stained with CDK6 antibody (ab124821, Abcam). IHC scores were conducted according to the ratio and intensity of positive-staining areas. The staining areas were scored as follow: 0-25%, score 1; 25-50%, score 2; 50-75%, score 3; and beyond 75%, score 4. The signal intensity was scored on a scale of 0-3: 0-negative, 1-

weak, 2-moderate and 3-strong. Two experienced pathologists scored the IHC staining independently and the final IHC score was the score average from both pathologists.

Cell lines and culture

Human CRC cell lines (HCT116 (RRID: CVCL_0291) and SW480 (RRID: CVCL_0546)) and normal human colon epithelial cell line NCM460 (RRID: CVCL_0460) were obtained from National Collection of Authenticated Cell Cultures (Shanghai, China). All human cell lines have been authenticated using STR profiling within the last three years and all experiments were performed with mycoplasma-free cells. These cell lines were maintained in Dulbecco's Modified Eagle Medium (Logan Utah, HyClone, USA) with 10% fetal bovine serum (FBS; Gibco), 1% penicillin (10 U/mL) and 1% streptomycin (10 μg/mL) in an incubator with the environment of 37 °C and 5% CO2.

Quantitative real-time polymerase chain reaction (qRT-PCR)

RNA was isolated with Trizol reagent. The purity and the concentration of different RNA samples were measured using NanoDrop ND-1000 (Thermo Scientific, USA). Reverse transcription reaction was performed using miRcute miRNA cDNA synthesis Kit (kr211, Tiangen, China) for miRNAs and SuperScript IV VILO cDNA synthesis kit (11756050, Thermo Scientific, USA) for mRNAs. Quantitative RT-PCR (qRT-PCR) was performed using SYBR® Premix Ex Taq™ (Takara) containing mRQ 3' Primer on an ABI 7500 platform (Applied Biosystems, Carlsbad, CA, USA). The relative quantities of miR-500a-3p in cells was normalized to U6. Beta actin was used as an internal control for mRNA detection. The primer sequences for miRNA and mRNA detection are listed in supplementary Table 3.

Lentivirus and miRNA transfection

The lentivirus overexpressing human miR-500a-3p and CDK6 was purchased from Genomeditech (Shanghai, China). miR-500a-3p mimics were synthesized by Genomeditech (Shanghai, China). The sequences of miR-500a-3p mimic were 5'-AUGCACCUGGGCAAGGAUUCUG-3'. The miRNA oligonucleotides were transfected using Lipofectamine® RNAiMAX™ (50 nmol/L; Invitrogen, CA, USA).

Cell viability assay

After 72 h lentivirus infection or 24 h miRNA transfection, HCT-116 (2,500/well) and SW480 (2000/well) cells were planted into 96-well culture plates. Cell viability was measured at 24, 48, 72 and 96h post seeding, by using the Cell Counting Kit-8 (Dojindo, Kumamoto, Japan) according to the manufacturer's instructions.

Colony-formation assay

HCT-116 (1500/well) and SW480 (2000/well) cells were seeded in six-well plates after 72 h lentivirus infection. The culture medium was changed every 3 days. After incubating for 2 weeks, colonies were

fixed with 4% paraformaldehyde for 15 min and stained with 5% Giemsa for 20 min. The colonies containing at least 50 cells were scored.

Cell cycle analysis

Seventy-two hours after infection, cells were harvested, washed with phosphate-buffered saline (PBS), and fixed in 70% ethanol at 4°C overnight. After fixation, cells were washed with PBS before suspension in RNase A/propidium iodide solutions (100 mg/mL RNase A and 5 μg/mL propidium iodide). Cells were incubated at room temperature for an hour. Stained cells were analyzed by a FACScan flow cytometer (BD Biosciences, Mountain View, CA, USA).

Cell apoptosis analysis

Cell apoptosis was assessed by annexin V/propidium iodide (BD Biosciences, San Jose, CA, USA). Cells were harvested, washed with PBS, and resuspended in 1× binding buffer at a concentration of 1×10^6 cells/mL. A total of 100 μL solution was transferred to a new tube and added with 5 μL of APC Annexin V and 5 μL of propidium iodide. Cells were incubated at room temperature for 15 min in the dark and then analyzed by a FACScan flow cytometer.

Cell invasion assay

The cell invasion assay was performed in 24-well transwell chambers pre-coated with Matrigel (Corning, NY, USA). HCT-116 cells (10^5/well) in 200 μL serum-free medium were seeded into the upper chamber, and 600 μL complete medium (with 10% FBS) was filled into the lower chamber. Cells on the inner membrane were removed with a cotton swab after 24 h. The outer membrane was fixed in 4% formaldehyde (in PBS) and stained with 0.5% crystal violet. Cell numbers were counted and averaged in five random fields at a magnification of 100×.

Xenograft tumor assay

BALB/c nude mice (6 weeks old) were purchased from Shanghai SLAC Laboratory animal co. ltd (shanghai, China) and randomly divided into 2 groups (n = 7/6). SW480 (3×10^6) or HCT116 (4×10^6) cells that stably transfected with miR-NC or miR-500a-3p were injected at the back region of BALB/c mice subcutaneously. The volume of tumors was measured twice a week using a vernier caliper with the method of volume = (length × width^2)/2. The mice were killed after inoculation for 30 d, and the tumors were weighed. Tumor tissues were subjected to

measure the expression of ki67. The procedures in this study were permitted by the Animal

Research Committee of the Zhongshan Hospital, Fudan University.

Luciferase reporter assay

The putative miR-500a-3p binding sequence and the matching mutant binding sequence in the 3'untranslated region (3'UTR) of CDK6 were amplified and inserted to pGL3 luciferase reporter vector (Genomeditech, shanghai, China). SW480 cells were transfected with miR-NC or miR-500a-3p and the above constructed reporter plasmids. After transfection for 48 h, the luciferase activities in different groups were determined by the dual-luciferase reporter assay system (Promega).

Glucose, lactate and ATP measurement

SW480 and HCT116 cells were cultured with FBS-free medium and culture medium was collected after 24h. Glucose Uptake Colorimetric Assay kit (Biovision, Milpitas, California, USA), Lactate Assay Kit (Biovision) and ATP Colorimetric Assay kit (Biovision) were utilized to detect the glucose consumption, the lactate production and ATP in CRC cells according to the manufacturer's instructions. The glucose, lactate and ATP levels were normalized to total cell protein.

Seahorse analysis

Extracellular acidification rate (ECAR) was detected using a Seahorse XF96 analyzer (Seahorse Biosciences, USA). SW480 cells (10^5/well) were seeded in a 96-well XF96 microplate (Seahorse Biosciences, USA). Before experiments, cell culture medium was replaced and cells were then incubated with assay medium for 1 h at 37 °C in a CO2-free incubator. ECAR was detected using sequential injection of 10mM glucose, 2mM oligomycin (Sigma-Aldrich) and 50mM 2-deoxyglucose (2-DG, Sigma-Aldrich). Each cycle of measurement involved mixing (3 min), waiting (2 min), and measuring (3 min) cycles.

Mass Spectrometry

The targeted metabolomics analyses were performed using an HPLC system (Agilent 1290, Agilent Technologies) and mass spectrometer (Agilent 5500, Agilent Technologies). A 10-cm dish of cultured tumor cells were collected, adding 1 ml acetonitrile / methanol water (v, 2:2:1) and storing at -80℃ after quick freezing in liquid nitrogen. Sample preparation processes were performed in accordance with the above method of parallel preparation of QC samples. MRM transitions representing the metabolites were simultaneously monitored, and the positive/negative polarity switching was used. Data analyses were performed as instructions by Shanghai Applied Protein Technology[17].

Western-blot

Whole protein extracts were lysed by radioimmunoprecipitation assay (RIPA) buffer (Thermo Fisher Scientific) according to the manufacturer's protocol. At that time, 30 μg proteins were run on a 10% sodium dodecyl sulfate poly-acrylamide gel electrophoresis (SDS-PAGE) gel at 100 V for 2 h and transferred to a polyvinylidene fluoride membrane at 80 V for 2 h. Membranes were blocked with 5% bovine serum albumin (BSA) in Tris buffered saline with Tween-20 (TBST) at room temperature for 1 h. They were then incubated overnight at 4°C with one of the following primary antibodies: anti-CDK6 (ab124821, Abcam) (1:1000), anti-GLUT1 (ab115730, Abcam) (1:1,000) and anti-HK2 (2867T, Cell

Signaling Technology) (1:1,000) and anti-beta actin (1:1,000) from Santa Cruz Biotechnology (Dallas, Texas, USA). After washing with TBST, membranes were incubated with secondary antibodies for 1 h at room temperature and signals were developed using an enhanced chemiluminescence kit (Pierce, Waltham, MA, USA).

Statistical analysis

SPSS (version 22.0, SPSS Inc.) or GraphPad Prism software (version 7.0, USA) were used to analyze the data and generate the graphs. The differences between the miR-500a-3p expression and the clinical characteristics of CRC patients were analyzed using $\chi 2$ test. Survival curves were generated using the Kaplan-Meier method and log-rank tests. Univariate and multivariate Cox regression analyses were conducted to identify the independent factors. The correlation among the expression of miR-500a-3p, CDK6 and HK2 was analyzed using Spearman's correlation test. Student's t-test or the Mann–Whitney U test were used to calculate the *P* value between two groups. $P < 0.05$ was identified as statistically significant. R software 3.5.1 was applied in this study for the statistical analyses. All miRNAs expression data were normalized.

Discussion

Investigating new prognosis biomarkers and uncovering the mechanism behind the progression of CRC are critical for CRC treatment. In the current study, we focused on the role of miR-500a-3p in CRC progression. We found that patients with low miR-500a-3p expression had worse prognosis and it was an independent prognostic factor for CRC patients. Further in vitro and in vivo experiments showed that miR-500a-3p inhibits CRC cell proliferation and aerobic glycolysis and discovered a novel target of it, CDK6. These data suggested that miR-500a-3p might serve as a novel prognostic biomarker or therapeutic target of CRC.

Accumulating evidence indicates that miRNAs contribute to CRC progression[18–20]. However, studies screening miRNAs from the sequencing results of large cohorts were relatively rare. We analyzed miRNAs that are significantly related to the prognosis of CRC from the cBioportal database and found that miR-500 has the most significant correlation with the prognosis of CRC patients (with the smallest p-value). Then we focused on miR-500a-3p whose role has not been reported in CRC.

Interestingly, both tumor-promoting and tumor suppressive roles of miR-500a-3p have been revealed. In hepatocellular carcinoma and gastric carcinoma, miR-500a-3p served as a tumor promoter via regulating the cancer cell stemness[10, 11]. While in non-small cell lung cancer, miR-500a-3p acts as a tumor suppressor via down-regulation of LY6K expression[21]. The diverse roles of miR-500a-3p might due to the heterogeneity of tumor. In this study we provide new evidence that miR-500a-3p served as a tumor suppressor at least in CRC and more importantly, for the first time, reveal the role of miR-500a-3p on cancer cell metabolism. Specifically, we found miR-500a-3p down-regulated the expression of glycolytic enzyme and inhibited glycolysis. Decreased glycolysis restrains the cellular buildings for rapid cell proliferation[4], and ultimately contributes to the tumor suppressive roles of miR-500a-3p in CRC.

Previous studies have shown that CDK6 is regulated by several miRNAs, such as miR-29b, miR-211 and miR-497[22–24]. Our study enriched the system in which CDK6 is regulated by miRNAs. We identified that CDK6 was a direct functional target of miR-500a-3p in CRC and found that miR-500a-3p could inhibit the transcription of CDK6. In different tumors, CDK6 regulates different key enzymes and plays a distinct role in glycolysis. Wang et al. found that CDK6 inhibits the glycolytic pathway and re-directs the glycolytic intermediates into the pentose phosphate pathway (PPP) and serine pathways[16]. Xing et al. proved that CDK6 promotes glycolysis via phosphorylation of the fructose bisphosphate PFK2 (PFKFB3) in breast cancer[25]. In this study, we found that CDK6 enhanced glycolysis in CRC and HK2 might be a potential downstream target of CDK6.

The inhibition of glycolysis by miR-500a-3p could only be partially restored by CDK6 overexpression, indicating other targets might also be involved in miR-500a-3p-mediated influence on glycolysis. Some reported targets of miR-500a-3p, such as XBP1 and FBXW7, could regulate glycolysis directly or indirectly[10, 26–28]. But there is no direct evidence on whether the inhibition of glycolysis by miR-500a-3p depend on them, and further study is needed.

Conclusion

Taken together, miR-500a-3p was found to be a tumor suppressor in CRC. miR-500a-3p blocked the proliferation, cell cycle and glycolysis of CRC cells via targeting CDK6. These findings will expand our understanding of the versatile role of miR-500a-3p in CRC progression and support the rational of miR-500a-3p in CRC treatment.

Abbreviations

CRC, colorectal cancer; qPCR, quantitative real-time PCR; IHC, immunohistochemistry; CCK-8, cell counting kit 8; miRNAs, MicroRNAs; CDK6, cyclin-dependent kinases 6; SUV, Standard Uptake Value; FACS, fluorescence-activated cell sorting; ECAR, extracellular acidification rate; PPP, pentose phosphate pathway; HK2, hexokinase2.

Declarations

• Ethics approval and consent to participate

The study was approved by the ethics committee of Fudan University Zhongshan Hospital and was performed according to Good Clinical Practice guidelines and the Declaration of Helsinki. Written informed consent was obtained from every patient.

• Consent for publication

Consent for publication was obtained from every patient

• Competing interests

No conflict of interest exits in the submission of this manuscript.

• Availability of data and materials

All data generated or analysed during this study are included in this published article and its supplementary information files.

• Funding

Supported by The National Natural Science Foundation of China (81602035, 81472228, 82072653); The Shanghai Municipal Health Commission: Shanghai Outstanding Youth Specialist Training Program (Q2017-059); Clinical Science and Technology Innovation Project of Shanghai (SHDC12016104); Shanghai Engineering Research Center of Colorectal Cancer Minimally Invasive (17DZ2252600); Youth fund of Zhongshan Hospital (2019ZSQN28).

• Authors' contributions

* YL, WT and LR contributed equally to this work. YL, WT and JX designed the study, and were involved in patients' management. YL and WT performed molecular biology assays. MY and YC performed the bioinformatics analysis, YW, LR and YC helped in the study design and revised the manuscript. TL, and MJ performed the statistical analyses. YL wrote the manuscript. WT and GC critically reviewed and revised the manuscript. All authors have read and approved the final version of the manuscript.

• Acknowledgements

Not applicable

References

1. Sung, H., et al., *Global Cancer Statistics 2020: GLOBOCAN Estimates of Incidence and Mortality Worldwide for 36 Cancers in 185 Countries.* CA Cancer J Clin, 2021. **71**(3): p. 209-249.
2. Brenner, H., M. Kloor, and C.P. Pox, *Colorectal cancer.* Lancet, 2014. **383**(9927): p. 1490-1502.
3. He, L. and G.J. Hannon, *MicroRNAs: small RNAs with a big role in gene regulation.* Nat Rev Genet, 2004. **5**(7): p. 522-31.
4. Vander Heiden, M.G., L.C. Cantley, and C.B. Thompson, *Understanding the Warburg effect: the metabolic requirements of cell proliferation.* Science, 2009. **324**(5930): p. 1029-33.
5. Vaupel, P., H. Schmidberger, and A. Mayer, *The Warburg effect: essential part of metabolic reprogramming and central contributor to cancer progression.* Int J Radiat Biol, 2019. **95**(7): p. 912-919.

6. Zhang, L.F., S. Jiang, and M.F. Liu, *MicroRNA regulation and analytical methods in cancer cell metabolism.* Cell Mol Life Sci, 2017. **74**(16): p. 2929-2941.
7. Li, S., et al., *lncARSR sponges miR-34a-5p to promote colorectal cancer invasion and metastasis via hexokinase-1-mediated glycolysis.* Cancer Sci, 2020. **111**(10): p. 3938-3952.
8. Wang, X., et al., *Exosome-delivered circRNA promotes glycolysis to induce chemoresistance through the miR-122-PKM2 axis in colorectal cancer.* Mol Oncol, 2020. **14**(3): p. 539-555.
9. Cai, B., et al., *Inhibition of microRNA-500 has anti-cancer effect through its conditional downstream target of TFPI in human prostate cancer.* Prostate, 2017. **77**(10): p. 1057-1065.
10. Lin, H., et al., *Exosomal MiR-500a-3p promotes cisplatin resistance and stemness via negatively regulating FBXW7 in gastric cancer.* J Cell Mol Med, 2020. **24**(16): p. 8930-8941.
11. Jiang, C., et al., *miR-500a-3p promotes cancer stem cells properties via STAT3 pathway in human hepatocellular carcinoma.* J Exp Clin Cancer Res, 2017. **36**(1): p. 99.
12. Jiang, M., et al., *Down-regulation of miR-500 and miR-628 suppress non-small cell lung cancer proliferation, migration and invasion by targeting ING1.* Biomed Pharmacother, 2018. **108**: p. 1628-1639.
13. Tang, W., et al., *MicroRNA-500a-5p inhibits colorectal cancer cell invasion and epithelial-mesenchymal transition.* Int J Oncol, 2020. **56**(6): p. 1499-1508.
14. Tang, W., et al., *The p300/YY1/miR-500a-5p/HDAC2 signalling axis regulates cell proliferation in human colorectal cancer.* Nat Commun, 2019. **10**(1): p. 663.
15. Nebenfuehr, S., K. Kollmann, and V. Sexl, *The role of CDK6 in cancer.* Int J Cancer, 2020. **147**(11): p. 2988-2995.
16. Wang, H., et al., *The metabolic function of cyclin D3-CDK6 kinase in cancer cell survival.* Nature, 2017. **546**(7658): p. 426-430.
17. Cai, Y., et al., *An integrated targeted metabolomic platform for high-throughput metabolite profiling and automated data processing.* Metabolomics, 2015. **11**(6): p. 1575-1586.
18. Zhuang, M., et al., *MALAT1 sponges miR-106b-5p to promote the invasion and metastasis of colorectal cancer via SLAIN2 enhanced microtubules mobility.* EBioMedicine, 2019. **41**: p. 286-298.
19. Sun, M., et al., *Integrated analysis identifies microRNA-195 as a suppressor of Hippo-YAP pathway in colorectal cancer.* J Hematol Oncol, 2017. **10**(1): p. 79.
20. Cao, L., et al., *MiR-760 suppresses human colorectal cancer growth by targeting BATF3/AP-1/cyclinD1 signaling.* J Exp Clin Cancer Res, 2018. **37**(1): p. 83.
21. Liao, X.H., Z. Xie, and C.N. Guan, *MiRNA-500a-3p inhibits cell proliferation and invasion by targeting lymphocyte antigen 6 complex locus K (LY6K) in human non-small cell lung cancer.* Neoplasma, 2018. **65**(5): p. 673-682.
22. Hoareau-Aveilla, C., et al., *miR-497 suppresses cycle progression through an axis involving CDK6 in ALK-positive cells.* Haematologica, 2019. **104**(2): p. 347-359.

23. Xia, B., et al., *miR-211 suppresses epithelial ovarian cancer proliferation and cell-cycle progression by targeting Cyclin D1 and CDK6.* Mol Cancer, 2015. **14**: p. 57.
24. Zhu, K., et al., *MiR-29b suppresses the proliferation and migration of osteosarcoma cells by targeting CDK6.* Protein Cell, 2016. **7**(6): p. 434-44.
25. Xing, Z., et al., *Expression of Long Noncoding RNA YIYA Promotes Glycolysis in Breast Cancer.* Cancer Res, 2018. **78**(16): p. 4524-4532.
26. Zhou, Y., et al., *lncRNA NEAT1 regulates gastric carcinoma cell proliferation, invasion and apoptosis via the miR-500a-3p/XBP-1 axis.* Mol Med Rep, 2021. **24**(1).
27. Wang, C., et al., *Fulvestrant inhibits the glycolysis of prolactinoma GH3 cells by downregulating IRE1/XBP1 signaling pathway.* Eur Rev Med Pharmacol Sci, 2018. **22**(16): p. 5364-5370.
28. Zhan, P., et al., *FBXW7 negatively regulates ENO1 expression and function in colorectal cancer.* Lab Invest, 2015. **95**(9): p. 995-1004.

Tables

Table 1: Correlation of miR-500a-3p expression with clinicopathologic characteristics in colorectal cancer

	miR-500a-3p expression		
Characteristics	**High (n=67)**	**Low (n=67)**	***P***
Gender			0.587
Male	42 (62.7)	45 (67.2)	
Female	25 (37.3)	22 (32.8)	
Age, year	61.0±13.0	63.6±10.0	0.227
Location			0.089
Right side	18 (26.9)	10 (14.9)	
Left side	49 (73.1)	57 (85.1)	
Tumor Size			**0.022**
<5cm	21 (31.3)	34 (50.7)	
≥5cm	46 (68.7)	33 (49.3)	
Differentiation			**0.043**
Well/Moderately	46 (68.7)	56 (83.6)	
Poor	21 (31.3)	11 (16.4)	
Depth of tumor			0.259
T1-T3	58 (86.6)	62 (92.5)	
T4	9 (13.4)	5 (7.5)	
Lymph node			0.119
Positive	31 (46.3)	40 (59.7)	
Negative	36 (53.7)	27 (40.3)	
Distant metastasis			0.825
Yes	55 (82.1)	54 (80.6)	
No	12 (17.9)	13 (19.4)	
TNM Stage			0.226
I-II	28 (41.8)	35 (52.2)	
III-IV	39 (58.2)	32 (47.8)	

Figures

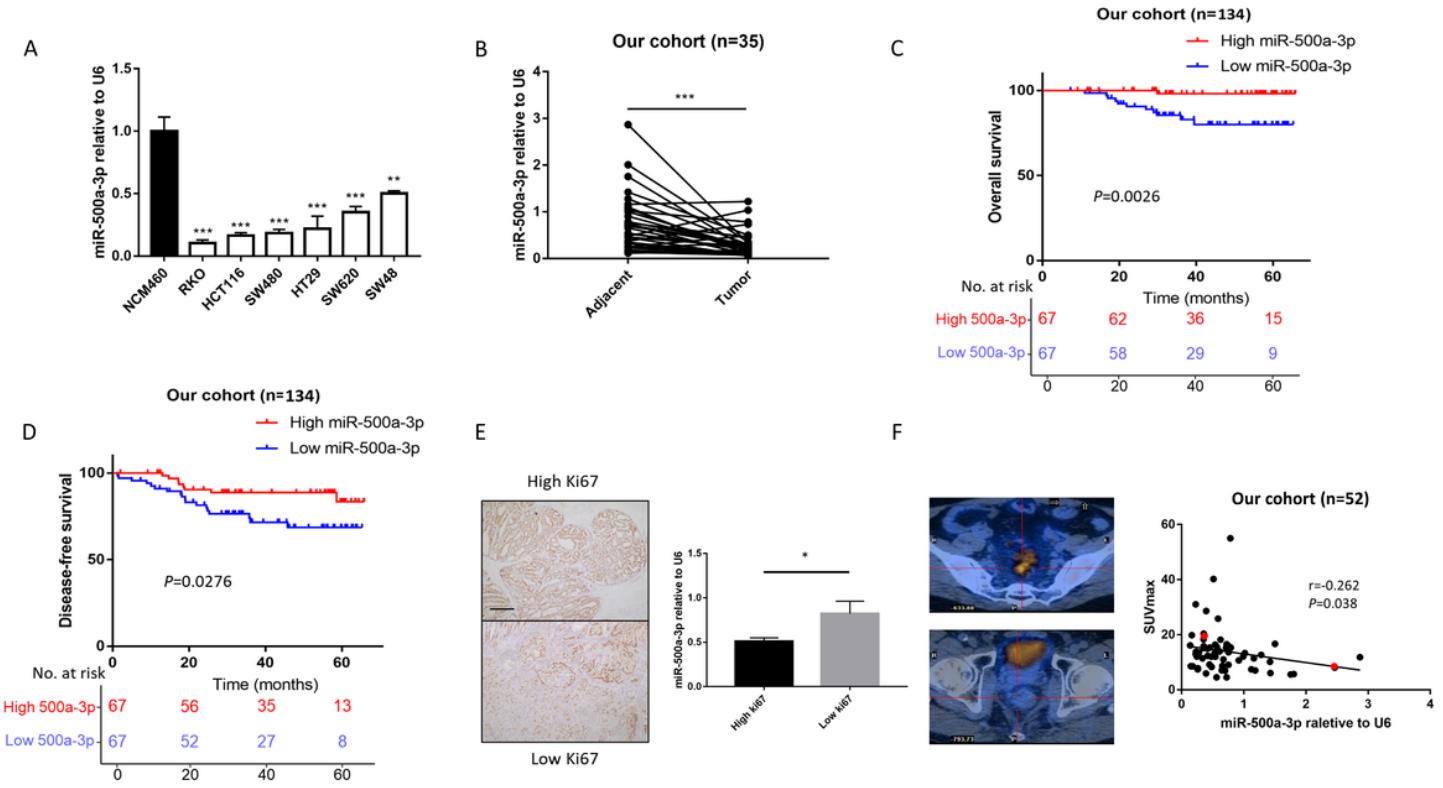

Figure 1

miR-500a-3p is down regulated in CRC and its low expression predicts poor prognosis (A) The enrichment of miR-500a-3p was determined in normal human colon epithelial cell line NCM460 and six CRC cell lines by RT-qPCR. (B) miR-500a-3p was upregulated in CRC tissues detected by qPCR in 20 pairs of CRC tissues (C-D) Low miR-500a-3p expression was significantly associated with poor overall survival (C) and disease-free survival (D) in CRC specimens. Median expression levels of miR-500a-3p were used as the cutoff. (E) The expression of miR-500a-3p was higher in low-ki67 group compared with high-ki67 group. Scale bar, 100 μm. (F) miR-500a-3p expression was negatively correlated with glucose uptake in CRC patients. Glucose uptake was represented by Standard Uptake Value of PET-CT. The left pictures show the PET-CT images of the patients indicated by the red dot.

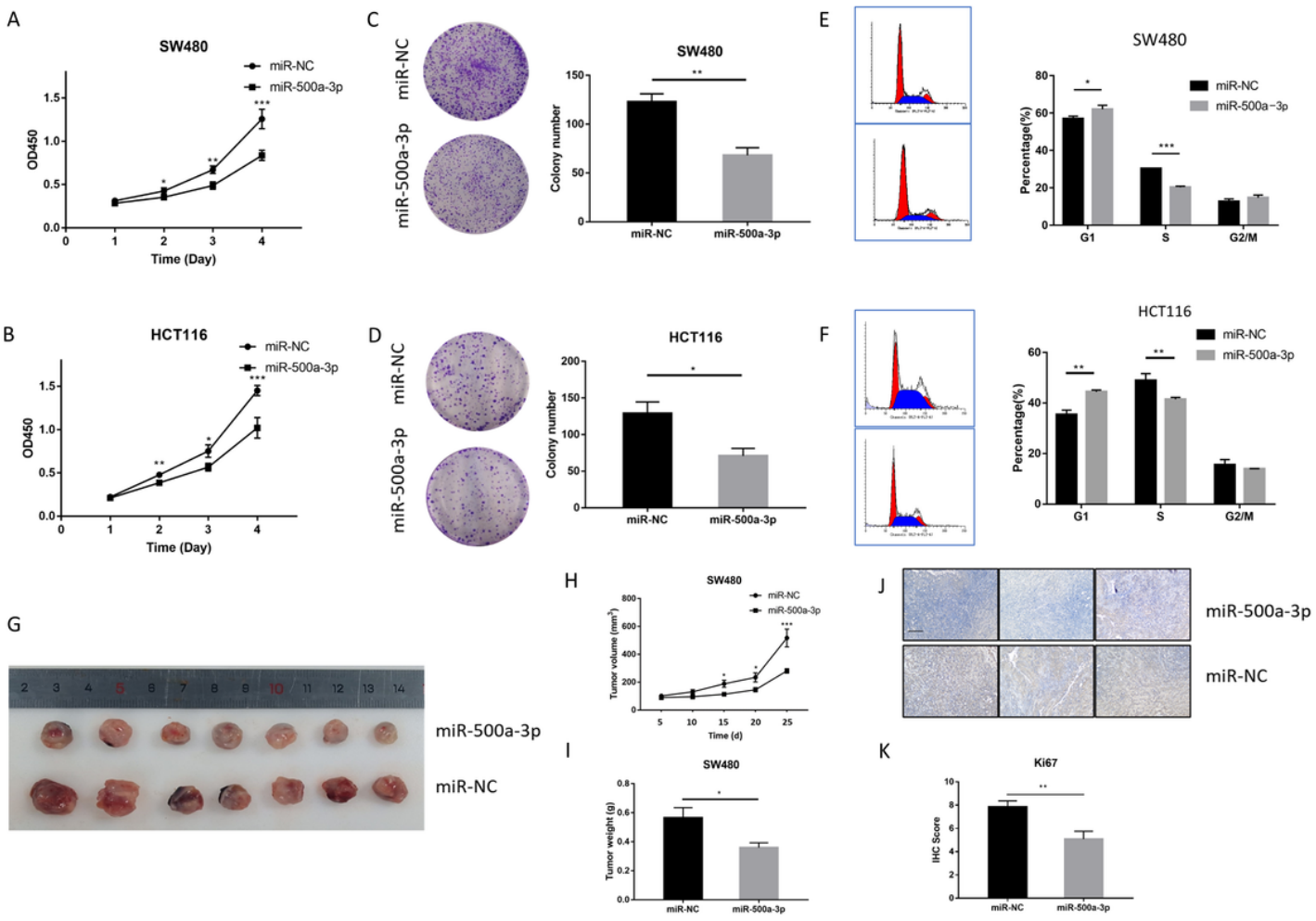

Figure 2

miR-500a-3p suppress CRC growth in vitro and in vivo (A-B) miR-500a-3p mimics significantly decreased cell proliferation compared with miR-NC cells using CCK-8 assay. (C-D) Colony numbers of HCT-116 and SW480 cells transfected with miR-500a-3p were significantly lower than in those transfected with miR-NC. (E-F) The cell cycle evaluated by flow cytometry showed that miR-500a-3p blocked cell cycle in G1 phase. (G) Representative tumor diagrams in different groups were shown. (H-I) Tumor volume and weight in the miR-500a-3p group were significantly lower than those in the miR-NC group. (J) Ki-67 expression was significantly higher in tumors of miR-500a-3p group than that of miR-NC group. Scale bar, 100 μm.

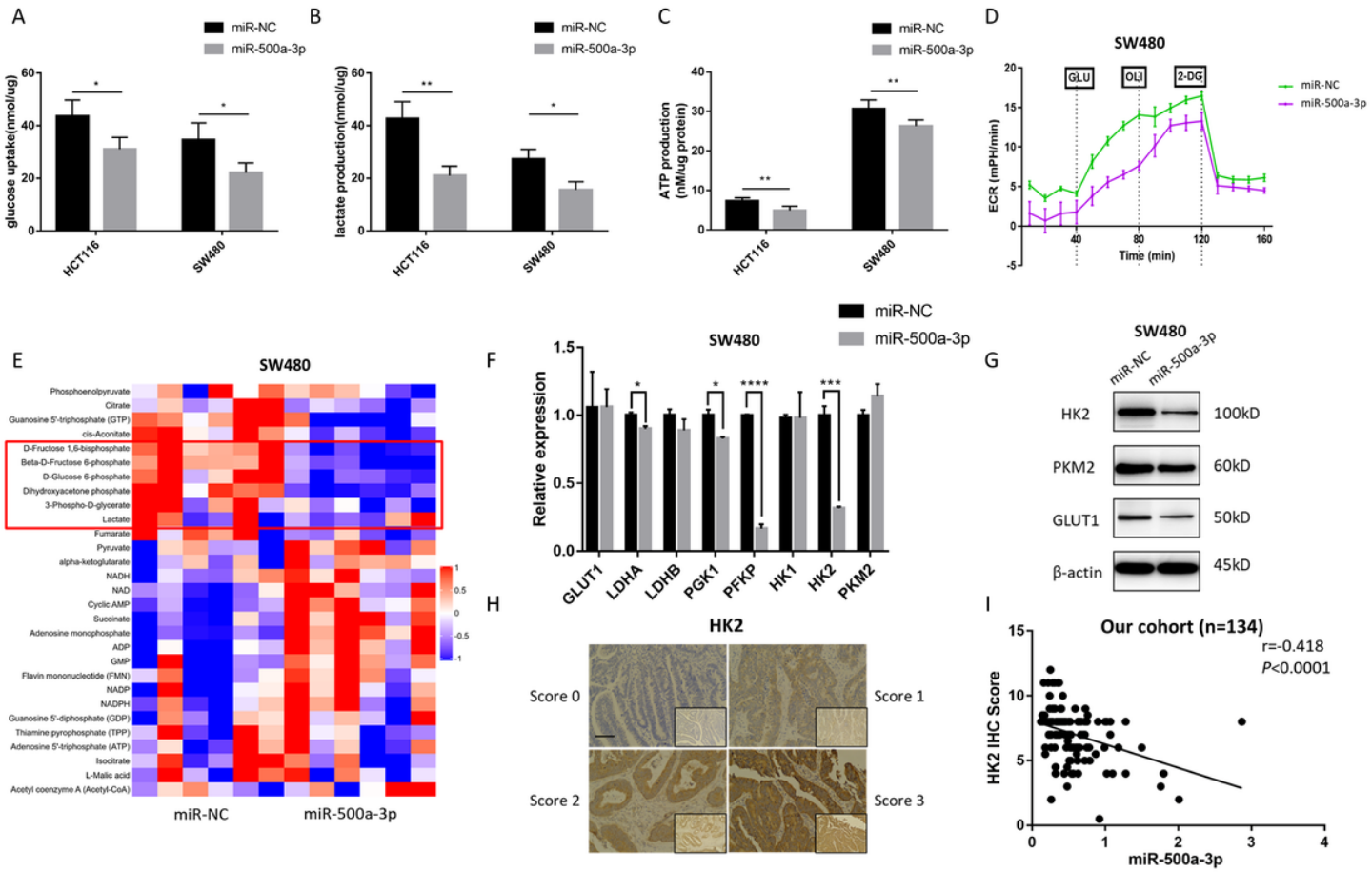

Figure 3

miR-500a-3p suppresses aerobic glycolysis in CRC (A-C) miR-500a-3p attenuated glucose uptake (A), lactate production (B), intracellular ATP (C) in HCT116 and SW480 cells. (D) The extracellular acidification rate (ECAR) of SW480 cells were analyzed by Seahorse XF96 Extracellular Flux Analyzer. (E) Heatmap showed overexpression of miR-500a-3p caused less level of glycolytic metabolites. (F-G) miR-500a-3p declined the mRNA level of HK2, PFKP, PGK1 and LDHA (F) and the protein level of GLUT1, HK2 and PKM2 (G). (H) Representative HK2 staining patterns. Scale bar, 100 μm. (I) Spearman correlation between miR-500a-3p and HK2 IHC score.

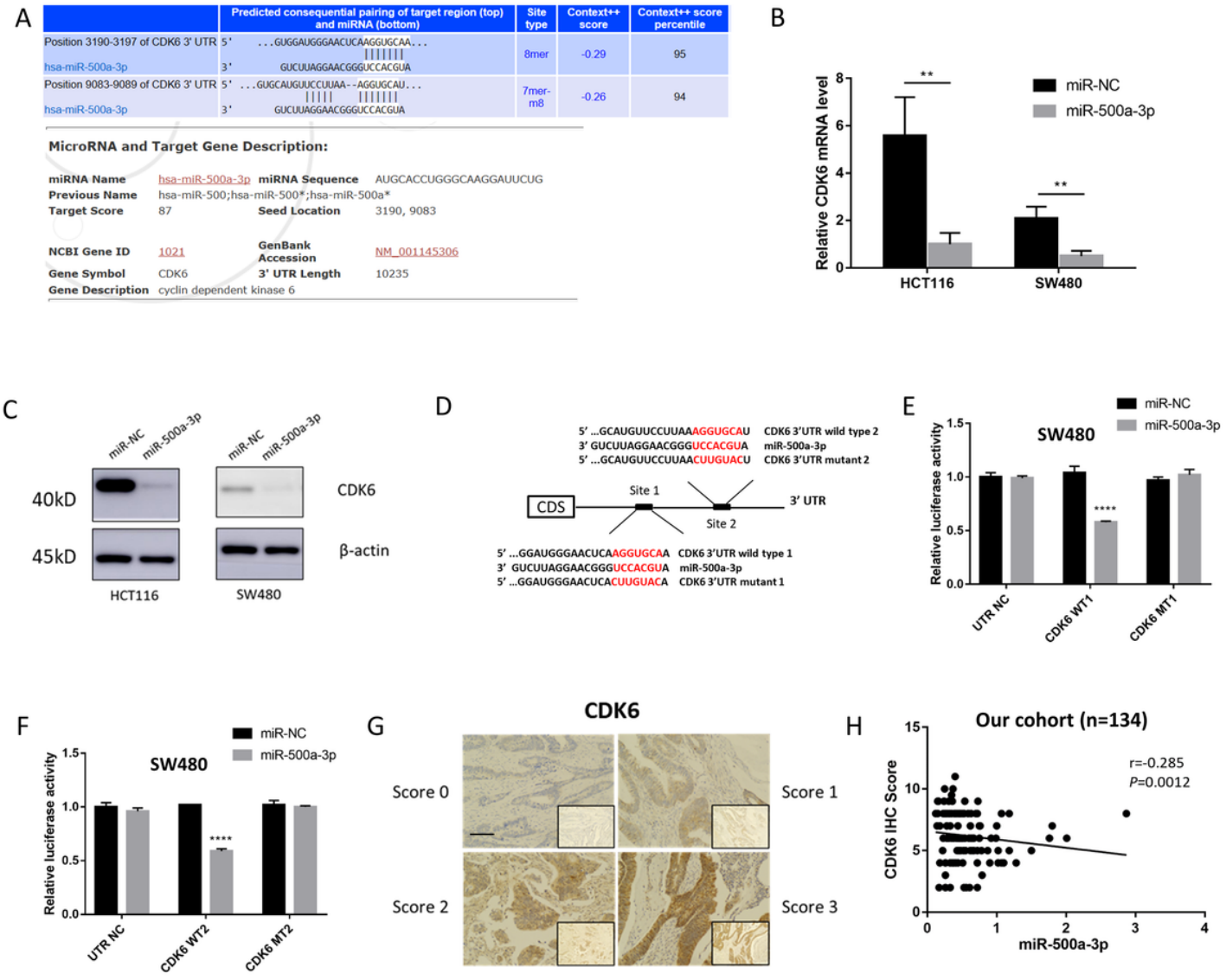

Figure 4

CDK6 is the direct target and down regulated by miR-500a-3p (A) Targetscan and miRDB predicted that two existed binding sites between miR-500a-3p and CDK6 mRNA. (B) CDK6 mRNA and protein levels after miR-500a-3p overexpression in HCT116 and SW480 cells. (C) CDK6 protein levels after miR-500a-3p overexpression in HCT-116, SW480 and HT29cells. (D) Schematic representation of luciferase reporter construct containing CDK6 3' UTR with either WT or mutant (MUT) miR-500a-3p target site. (E-F) Co-transfection of miR-500a-3p mimics and CDK6 3'UTR-wt strongly decreased the luciferase activity, while co-transfection of miR-500a-3p mimics and CDK6 3'UTR-mt did not change the luciferase activity. (G) Representative CDK6 staining patterns. Scale bar, 100 μm. (H) Spearman correlation between miR-500a-3p and CDK6 IHC score.

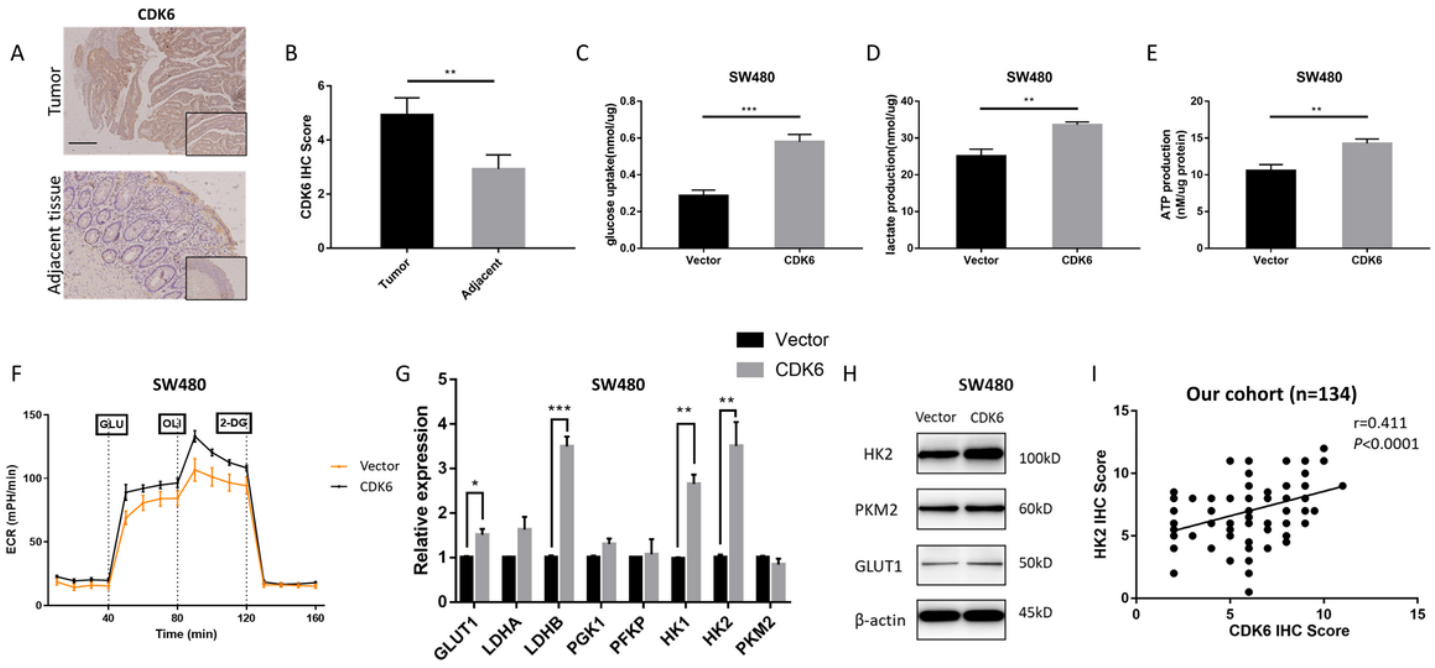

Figure 5

CDK6 is upregulated and promotes aerobic glycolysis in CRC (A-B) Expression level of CDK6 was higher in CRC tissues than in normal tissues by IHC staining. Scale bar, 100 μm. (C-E) CDK6 promoted glucose uptake (C), lactate production (D), intracellular ATP (E) in SW480 cells. (F) CDK6 overexpression enhanced the extracellular acidification rate (ECAR) of SW480 cells (G-H) miR-500a-3p declined the mRNA level of GLUT1, LDHB, HK1 and HK2 (G) and the protein level of GLUT1 and HK2 (H). (I) Spearman correlation between IHC score of CDK6 and HK2.

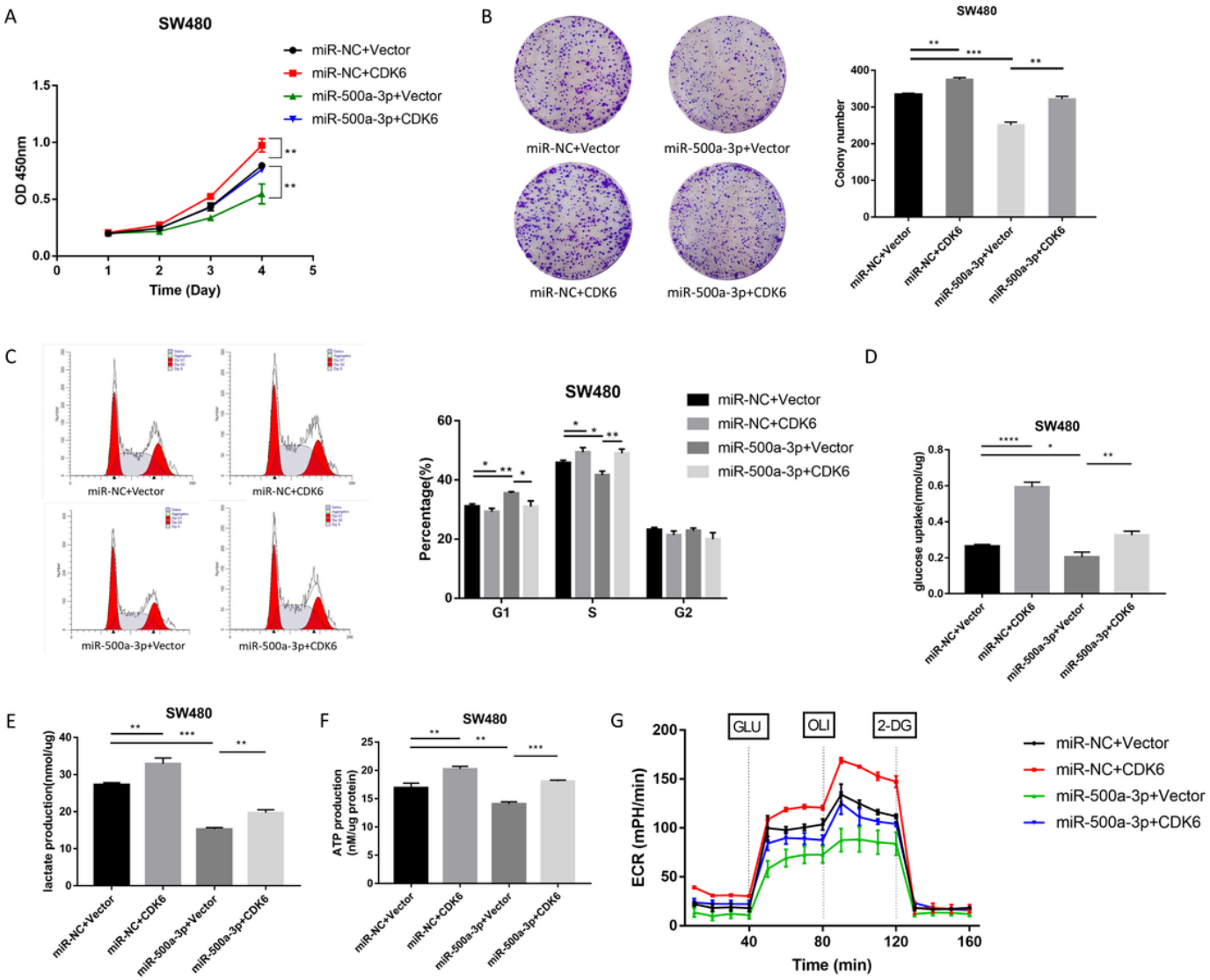

Figure 6

CDK6 overexpression recovers the proliferation and glycolysis of CRC cells which is restrained by the transfection of miR-500a-3p mimics (A) CCK-8 assay showed that the introduction of CDK6 reversed the proliferation-inhibiting effect of miR-500a-3p in CRC cells. (B) The introduction of CDK6 attenuated the colony formation inhibiting effect of miR-500a-3p in CRC cells (C) The cell cycle evaluated by flow cytometry showed that CDK6 attenuated the blockage at cell cycle G1 phase caused by miR-500a-3p. (D-F) The inhibition of glucose uptake (D), lactate production (E), intracellular ATP (F) induced by miR-500a-3p were partially attenuated after the introduction of CDK6. (G) Seahorse XF 96 Extracellular Flux Analyzer was used to detect the ECAR in four groups of CRC cells.

Supplementary Files

This is a list of supplementary files associated with this preprint. Click to download.

- SupplementalFigures.docx
- SupplementalTables.docx